

# Protective Effects of Total Flavonoids from *Lysimachia Christinae* on Calcium Oxalate-Induced Oxidative Stress in a Renal Cell Line and Renal Tissue

**Jian Wang**

The Second Clinical Medical College of Zhejiang Chinese Medical University

**Jiajian Chen**

The Second Clinical Medical College of Zhejiang Chinese Medical University

**Jiahao Huang**

The Second Clinical Medical College of Zhejiang Chinese Medical University

**Bodong Lv**

Zhejiang Chinese Medical University Affiliated Second Hospital

**Xiaojun Huang**

Zhejiang Chinese Medical University Affiliated Second Hospital

**Qing Hu**

Zhejiang Chinese Medical University Affiliated Second Hospital

**Jun Fu**

Zhejiang Chinese Medical University Affiliated Second Hospital

**Wenjie Huang**

Zhejiang Chinese Medical University Affiliated Second Hospital

**Tingting Tao** (✉ [aprilssunny@163.com](mailto:aprilssunny@163.com))

The Second Affiliated Hospital of Zhejiang Chinese Medical University

---

## Research

**Keywords:** kidney stones, calcium oxalate, flavonoids, oxidative stress, Nrf2/ARE

**Posted Date:** December 23rd, 2020

**DOI:** <https://doi.org/10.21203/rs.3.rs-132214/v1>

**License:**  This work is licensed under a Creative Commons Attribution 4.0 International License.

[Read Full License](#)

---

# Abstract

**Background:** Flavonoids are compounds with 2-phenylchromone as the basic mother nucleus and are natural antioxidant components of *Lysimachia christinae*. We previously demonstrated that total flavonoids from *L. christinae* (TFL) reduce calcium and oxalic acid concentrations in urine and can reduce oxidative stress (OS) in renal tissue, thus, inhibiting calcium oxalate (CaOx) stone formation. The aim of this study was to investigate whether TFL reduced OS in renal tissue, thereby inhibiting CaOx stone formation through the nuclear factor-E2 related factor 2 (Nrf2)/antioxidant response element (ARE) pathway.

**Methods:** The rat model of CaOx stone was established by providing rats with drinking water containing 0.5% glycol and 2% ammonium chloride. After 4 weeks of treatment with different doses of TFL (62.5, 125, and 250 mg/kg/d), body and kidney weights of the rats were measured. CaOx crystal formation was observed under the microscope and the renal tissue contents of superoxide dismutase (SOD) and malondialdehyde (MDA) were analyzed. HK-2 cells were divided into two groups: treatment with CaOx crystals or CaOx crystals + TFL. Other HK-2 cells were treated with small interfering RNA targeting nuclear factor-E2 related factor 2 (Nrf2) and divided into the same two groups. The activities of SOD and content of MDA were measured. The expression of Nrf2, heme oxygenase (HO-1), and NAD(P)H quinone oxidoreductase 1 (NQO-1) were detected using western blot.

**Results:** In the in vitro study, TFL significantly increased nuclear Nrf2 and expression of the downstream antioxidant genes, HO-1 and NQO-1. Furthermore, TFL increased superoxide dismutase activity and decreased the malondialdehyde content, thereby alleviating OS in renal tubular epithelial cells. Moreover, silencing the expression of Nrf2 blocked the protective effect of TFL on CaOx-induced OS. In the in vivo study TFL protected the renal cell line and renal tissue against injury, reduced CaOx-induced OS in renal tissue, and reduced CaOx crystal formation.

**Conclusions:** TFL reduces CaOx-induced OS in renal tissue by activating the nuclear Nrf2/antioxidant response element (ARE) pathway.

## 1. Introduction

Calcium oxalate (CaOx) stones account for more than 70% of renal calculi<sup>1</sup>. The causes of urinary stones are extremely complex. It is generally believed that urinary stone formation is not caused by a single factor, but a joint action of genetic, environmental, dietary, and metabolic factors<sup>2,3</sup>. Several studies have shown that renal tubule epithelial cell (RTEC) injury may be a key factor causing the formation of renal calculi<sup>4,5</sup>. RTEC injury leads to changes in the structure of the cell membrane. This provides an effective site for calcium salt crystal adhesion, and promotes the deposition and aggregation of crystals into stones<sup>6,7</sup>. Further, RTECs exposed to high concentrations of oxalic acid or CaOx crystals can produce abundant reactive oxygen species (ROS), and have reduced superoxide dismutase (SOD) and catalase activities, which can cause oxidative stress (OS), even leading to RTEC apoptosis and death<sup>8</sup>. ROS-

induced RTEC injury and subsequent OS are closely related to the formation of renal calculi and may even be an important initiating event. Therefore, we speculated that reducing OS in renal tissue may prevent the formation and recurrence of renal calculi.

OS is the result of an imbalance between intracellular pro-oxidant and antioxidant defense systems. When the intracellular antioxidant capacity is insufficient or weakened, OS occurs<sup>9,10</sup>. Nuclear factor (NF)-E2 related factor 2 (Nrf2)/antioxidant response element (ARE) is an important endogenous anti-OS signaling pathway and is a major regulatory factor of antioxidant resistance<sup>10,11</sup>. Several studies have shown that the absence of Nrf2, or functional damage to Nrf2, can aggravate OS, while Nrf2 activators can prevent kidney disease progression by protecting cells from oxidative damage<sup>12,13</sup>. The Nrf2 activator, dimethyl fumarate, can alleviate calcium deposition and renal tissue injury induced by hyperoxaluria in rats, and downregulate the expression of bone morphogenic protein 2 and osteopontin<sup>14</sup>.

Flavonoids are compounds with 2-phenylchromone as the basic mother nucleus. These molecules are important natural antioxidants and are the main active components in *Lysimachia christinae*<sup>15,16</sup>. Indeed, flavonoids have high efficacy and low toxicity in the prevention and treatment of ROS-associated diseases. Some flavonoids act as antioxidants and Nrf2 activators, which activate the Nrf2 signaling pathway<sup>17</sup>. *In vitro* cell experiments showed that total flavonoids from *Lysimachia christinae* (TFL) protected against cell damage induced by CaOx crystals. Our previous study demonstrated that TFL reduced calcium and oxalic acid concentrations in the urine, thus inhibiting CaOx stone formation<sup>18</sup>. We also confirmed that TFL can reduce OS in renal tissue<sup>19</sup>. Therefore, the specific mechanism underlying TFL inhibition of CaOx stone formation is worthy of further investigation.

Here, we investigated whether TFL reduced renal tissue OS induced by CaOx stone formation via Nrf2/ARE pathway activation. We hypothesized that Nrf2/ARE activation would prevent CaOx stone formation. We showed that TFL reduced OS in renal tissue induced by CaOx accumulation, and reduced CaOx crystal formation. Importantly, we confirmed that TFL significantly increased the nuclear Nrf2 content and hemeoxygenase-1 (HO-1) and NAD(P)H quinone oxidoreductase 1 (NQO-1) protein expression in HK-2 cells treated with CaOx crystals. In addition, TFL treatment significantly increased SOD activity and decreased malondialdehyde (MDA) content in HK-2 cells, thereby reducing OS in RTECs. Silencing Nrf2 expression blocked the protective effect of TFL on CaOx-induced OS. Thus, TFL reduces CaOx-induced OS in renal tissue by activating the Nrf2/ARE pathway.

## 2. Materials And Methods

### 2.1. Reagents and antibodies

TFL (20%) was purchased from DASF (Nanjing, China). Ethylene glycol and ammonium chloride were purchased from Sinopharm (Beijing, China). Calcium oxalate, RIPA lysis solution, Tris buffer, diphenyliodonium (DPT), 3-(4,5-dimethylthiazol-2-yl)-2,5-diphenyltetrazolium bromide tetrazolium (MTT), and dimethyl sulfoxide(DMSO) were obtained from Sigma-Aldrich (USA). Penicillin, fetal bovine

serum, and streptomycin were purchased from Gibco (USA). Antibodies against Nrf2, HO-1, and NQO-1 were obtained from Abcam (USA). Horseradish peroxidase-conjugated secondary antibodies were acquired from Bio-Rad (USA). Bicinchoninic acid(BCA) protein assay and total superoxide dismutase (WST-8) and lipid peroxidation malondialdehyde (MDA) assays, and nuclear and cytoplasmic protein extraction kits were purchased from Beyotime (Shanghai, China). Polyvinylidene difluoride membranes were purchased from EMD Millipore (USA). Annexin V-FITC/PI kits were purchased from Solarbio. Lipofectamine 2000 reagent was purchased from Thermo Fisher (USA).

## 2.2. Animal experiments

All animal experiments were approved by the Animal Experimental Ethics Committee of Zhejiang Chinese Medical University. Fifty adult male Sprague-Dawley rats (250–300 g) were purchased from the Laboratory Animal Center of Zhejiang Chinese Medical University. All rats were housed in cages at 20–25 °C and 40–60% humidity, under a 12 h light/dark cycle. Rats were weighed and divided randomly into five groups: normal control (NC); CaOx stone model (M), rats treated with 0.5% glycol and 2% ammonium chloride (1 ml/rat/d) in drinking water; CaOx stone model + low-dose TFL (LT) (62.5 mg/kg/d TFL); CaOx stone model + medium-dose TFL (MT) (125 mg/kg/d TFL); and CaOx stone model + high-dose TFL (HT) (250 mg/kg/d TFL). Each group was treated for 28 days. At the end of the experiment, the rats were weighed. After being anesthetized with intraperitoneal pentobarbital, the kidneys were quickly excised, weighed, fixed in 4% paraformaldehyde solution, frozen in liquid nitrogen, and stored at – 80 °C. Renal hypertrophy was assessed using the kidney/body weight ratio.

## 2.3. Histopathologic scoring

Kidney cortex samples were fixed in 4% paraformaldehyde, embedded in paraffin, serially sectioned (4 μm thickness), and stained with hematoxylin/eosin. Ten visual fields from each section were observed under a microscope at 100 × magnification. The degree of crystallization and renal tubular dilatation were scored for each visual field, and the average crystallization and dilation scores were calculated. The scoring criteria for crystallization were as follows: 0, no crystals; 1, few crystals (one or two per field); 2, moderate number of crystals (10–20 per field); and 3, high number of crystals ( $\geq 20$  per field). Renal tubule dilation was scored as follows: 0, no obvious expansion; 1, scattered mild expansion; 2, extensive mild expansion, with scattered moderate expansion; 3: extensive moderate expansion, with scattered severe expansion; and 4: extensive severe expansion.

## 2.4. Small interfering (si)RNA transfection

SiRNA sequences targeting the Nrf2 gene, and scrambled siRNA negative controls, were purchased from Sangon Biotech (Shanghai, China). The Nrf2-siRNA sequence was 5'-GCCUGUAAGUCCUGGUCAUTT-3', and the nonspecific negative control siRNA sequence was 5'-UUCUCCGAACGUGUCACGUTT-3'. Transient transfections were performed using the Lipofectamine 2000 transfection reagent.

## 2.5. Cell culture

Human proximal tubular cells (HK-2 cells) were provided by the Laboratory Animal Center of Zhejiang Chinese Medical University (Hangzhou, China). The cells were maintained in Dulbecco's modified Eagle's medium containing 1 × penicillin-streptomycin and 10% fetal bovine serum (Gibco) at 37 °C. The cells were subcultured with 0.25% trypsin when they reached 80% confluency. Cells in the logarithmic growth phase were harvested and seeded in 6-well plates until they reached 70–80% confluence. Then, HK-2 cells were divided into seven groups: 1) normal control (NC), 2) CaOx crystal model (M, HK-2 cells were treated with 2 mM CaOx crystal suspension), 3) M + TFL (HK-2 cells were treated with 2 mM CaOx crystal suspension and 50 µg/ml TFL), 4) Nrf2 siRNA (HK-2 cells were transfected with NRF2-siRNA), 5) NC siRNA (HK-2 cells were transfected with control siRNA), 6) Nrf2 siRNA + M (HK-2 cells were transfected with NRF2-siRNA and then were treated with 2 mM CaOx crystal suspension), and 7) Nrf2 siRNA + M + TFL (50 µg/mL).

## 2.6. Cell viability assay

Cell viability was determined using the 3-(4,5-dimethylthiazol-2-yl)-2,5-diphenyltetrazolium bromide (MTT) assay. Briefly, HK-2 cells in the logarithmic phase were seeded at 100 µL per well in 96-well plates and incubated in an incubator at 37 °C with 5% CO<sub>2</sub>. After treatment, 20 µL of 5 mg/mL MTT was added to each well and the cells were incubated for 4 h at 37 °C. The supernatant was discarded and 150 µL of dimethyl sulfoxide was added to each well. The mixture was gently shaken on a mini shaker at room temperature for 10 min. Absorbance at 490 nm was measured on a microplate reader (Molecular Devices, USA). The percent viability of treated cells was calculated using the formula:

$$\text{viability (\%)} = (\text{OD}_{\text{treated}} - \text{OD}_{\text{blank}}) / (\text{OD}_{\text{negative control}} - \text{OD}_{\text{blank}}) \times 100.$$

## 2.7. Flow cytometric detection of apoptosis

Apoptotic cell death was determined using the Annexin V-FITC/PI Apoptosis Kit according to the manufacturer's instructions. Cells were analyzed using flow cytometry.

## 2.8. Oxidative stress

Renal MDA and total SOD levels of kidney tissue and HK-2 cells were determined using commercial kits (Beyotime) to evaluate the degree of oxidative stress.

## 2.9. Western blotting

Western blotting was performed to detect the expression of Nrf-2, HO-1, and NQO-1. HK-2 cells were lysed in RIPA lysis buffer containing 1% phenylmethylsulfonyl fluoride and centrifuged at 12,000 rpm for 15 min at 4 °C. The total protein concentration was determined using a BCA Protein Assay Kit. Cell membrane proteins and nucleoproteins were extracted using a Cell Cytoplasmic Protein/Nucleoprotein Extraction kit. After denaturation, proteins were separated by sodium dodecyl sulfate-polyacrylamide gel electrophoresis and transferred to polyvinylidene difluoride membranes. After blocking with Tris buffer solution containing 5% nonfat milk for 1 h at 25–30 °C, the membranes were incubated overnight at 4 °C with primary antibodies against Nrf2, HO-1 and NQO-1. After thorough washing, the blots were incubated

with a horseradish peroxidase-conjugated secondary antibody. Images were captured using an Odyssey two-color infrared laser imaging system (Li-Cor, Lincoln, NE, USA) and analyzed using Quantity One 1.62 software.

## 2.10. Statistical analyses

All data were analyzed using the SPSS 24.0 software. Normally distributed data are expressed as means  $\pm$  SEM. Analysis of variance was used for multiple comparison of data, followed by Fisher's *post hoc* least significant difference test. Tamhane's T2 tests were used for data with heterogeneous variances. Data that were not normally distributed are expressed as the median (*M (range)*), and the Wilcoxon rank sum test was used to compare these groups.  $P < 0.05$  was considered statistically significant.

## 3. Results

### 3.1 CaOx crystals reduce the viability and induce apoptosis of HK-2 cells.

HK-2 cells were treated with a CaOx crystal suspension (0.1, 0.25, 0.5, 1.0, 2.0, and 4.0 mM) for 24 h and apoptosis was detected by flow cytometry. The percentage of cells undergoing apoptosis in response to 0, 0.1, 0.25, 0.5, 1.0, 2.0, and 4.0 mM CaOx treatment was  $3.41 \pm 0.78$ ,  $8.48 \pm 0.32$ ,  $13.6 \pm 0.57$ ,  $21.2 \pm 0.85$ ,  $26.1 \pm 0.76$ ,  $35.4 \pm 0.62$ , and  $45.4 \pm 0.46$ , respectively (Fig. 1). The MTT assay showed that CaOx crystals decreased HK-2 cell viability in a concentration- as well as time-dependent manner (Fig. 2).

### 3.2 TFL protects HK-2 cells from damage induced by CaOx crystals

The percentages of cells undergoing apoptosis after 2 h pretreatment with TFL (0, 10, 25, 50, and 125  $\mu\text{g/ml}$ ) followed by treatment with a 2 mM CaOx crystal suspension for 24 h were  $27.4 \pm 5.00$ ,  $24.4 \pm 2.64$ ,  $17.3 \pm 2.34$ ,  $13.7 \pm 1.92$ , and  $12.3 \pm 2.20$ , respectively (Fig. 3). Apoptosis significantly decreased after pretreatment with 25, 50, and 125  $\mu\text{g/ml}$  TFL than the control group ( $P < 0.01$ ), but there was no significant difference between the 50 and 125  $\mu\text{g/ml}$  groups ( $P > 0.05$ ). The MTT assay showed that TFL treatment mitigated the damage to HK-2 cells induced by CaOx crystals, while cell survival increased gradually with increasing concentrations of TFL (Fig. 4). The survival of cells pretreated with 50 and 125  $\mu\text{g/ml}$  of TFL was significantly higher than that of the control group ( $P < 0.05$  and  $P < 0.01$ , respectively), but there was no significant difference between these two groups ( $P > 0.05$ ).

\*  $P < 0.05$ , \*\*  $P < 0.01$  vs. 0 mM oxalate group

\*  $P < 0.05$ , \*\*  $P < 0.01$  vs. 0 mM oxalate group

### 3.3 TFL reduces CaOx stone-induced OS *in vitro* and *in vivo*

SOD activity in CaOx crystal-treated HK-2 cells was significantly lower ( $P < 0.01$ ) than that in normal control HK-2 cells, and the MDA content was higher ( $P < 0.05$ ) (Fig. 6). This confirmed the presence of OS in CaOx crystal-treated HK-2 cells. After intervention with TFL, SOD activity was significantly increased ( $P < 0.01$ ) and the MDA content was markedly decreased ( $P < 0.01$ ) as compared to levels in CaOx crystal-treated HK-2 cells not exposed to TFL, indicating that TFL can reduce OS induced by CaOx crystals. *In vivo* experiments confirmed the *in vitro* results. As shown in Fig. 7, SOD activity in the kidney tissue of CaOx stone model rats was significantly lower ( $P < 0.01$ ) and the MDA content was higher ( $P < 0.05$ ) than those in the kidney tissue of control rats. After intervention with moderate and high TFL doses, SOD activity was significantly increased and the MDA content was decreased ( $P < 0.05$ ), as compared with levels in model rats.

### **3.4 TFL increases the nuclear Nrf2 content and downstream antioxidant gene expression in CaOx crystal-induced HK-2 cells**

Western blotting data showed that there was no significant difference in the expression of total Nrf2 protein between HK-2 cells treated with CaOx crystals and normal cells ( $P > 0.05$ ) (Fig. 8B). However, Nrf2 expression in nuclear extracts, and HO-1 and NQO-1 expression, were upregulated in CaOx crystal-treated HK-2 cells (Fig. 8D, E, and F). After intervention with TFL, nuclear Nrf2, HO-1, and NQO-1 expression was further increased, indicating that TFL could activate the Nrf2/ARE pathway.

### **3.5 Nrf2/ARE pathway is downregulated in HK-2 cells after Nrf2 siRNA treatment**

We first evaluated the Nrf2/ARE pathway by inactivating it with Nrf2 siRNA. After Nrf2 siRNA treatment, the Nrf2/ARE pathway was efficiently downregulated ( $P < 0.01$ ) in HK-2 cells as compared with NC Nrf2 siRNA treatment (Fig. 9B, C, and D). Along with decreasing Nrf2 levels, Nrf2 siRNA markedly reduced the HO-1 and NQO-1 protein levels ( $P < 0.01$ ) (Fig. 9E and F), indicating that we could effectively silence the expression of Nrf2 in cells and affect the expression of downstream genes by siRNA treatment. Importantly, Nrf2 siRNA treatment reversed the upregulated expression of nuclear Nrf2, HO-1, and NQO-1 induced by CaOx crystals in HK-2 cells (Fig. 8D, E, and F). The levels were even lower than those in the normal control group ( $p < 0.01$ ). Furthermore, after Nrf2 siRNA treatment, TFL did not show any effect on the expression of nuclear Nrf2, HO-1, NQO-1, in CaOx crystal-treated HK-2 cells.

### **3.6 Nrf2/ARE pathway mediates the effect of TFL on OS**

TFL treatment significantly increased SOD activity and significantly reduced the MDA content in HK-2 cells treated with CaOx crystals. TFL also increased nuclear Nrf2, and HO-1, and NQO-1 expression. However, Nrf2 siRNA treatment reversed the upregulated expression of nuclear Nrf2, HO-1, and NQO-1, induced by TFL in CaOx crystal-treated HK-2 cells (Fig. 4D, E, and F). As shown in Fig. 6, Nrf2 siRNA treatment also markedly decreased SOD activity ( $P < 0.01$ ) and increased the MDA content ( $P < 0.01$ ) in

CaOx crystal-treated HK-2 cells exposed to TFL. These results were not different from the results in HK-2 cells treated with Nrf2 siRNA and CaOx alone ( $P > 0.05$ ), indicating that there was no significant effect of TFL treatment on CaOx crystal-induced OS after Nrf2 siRNA treatment.

### 3.7 TFL inhibits the formation of renal calculi in a CaOx stone rat model

As shown in Table 1, CaOx stone model rats exhibited diminished body weight and a higher kidney weight/body weight ratio, which indicates kidney hypertrophy compared to normal rats. Hematoxylin/eosin staining showed broadly dilated kidney tubules and crystal deposition in the renal tubule lumen of CaOx stone model rats (Fig. 5); the crystallization score was  $2.30 \pm 0.26$  and the renal tubule dilation score was 3 (Table 1). These scores were significantly higher than those in the normal control group, which suggests that the CaOx stone rat model was successfully established. Rats in the high-dose TFL treatment group showed a reduced kidney weight/body weight ratio, a low degree of crystal formation, and a lower degree of renal tubule dilation than did CaOx stone model rats (Table 1). However, treatment with low- and medium-dose TFL did not show a significant effect.

Table 1  
Effect of TFL on the renal tissue of CaOx stone model rats

Parameters	NC	M	LT	MT	HT
BW loss (g)	$7.00 \pm 13.65$	$45.5 \pm 24.2^{**}$	$32.0 \pm 19.2^{**}$	$31.5 \pm 9.8^{**}$	$28.8 \pm 20.8^{**\#}$
KW (g)	$1.89 \pm 0.29$	$2.64 \pm 0.86^{**}$	$2.65 \pm 0.69^{**}$	$2.58 \pm 0.70^*$	$2.15 \pm 0.28$
KW/BW (%)	$0.69 \pm 0.09$	$1.07 \pm 0.40^{**}$	$1.09 \pm 0.26^{**}$	$0.95 \pm 0.21^*$	$0.84 \pm 0.10^{\#}$
SCD	$0.50 \pm 0.22$	$2.30 \pm 0.26^{**}$	$2.00 \pm 0.26^{**}$	$2.00 \pm 0.21^{**}$	$1.50 \pm 0.22^{**\#}$
SRTDD	0 (0-)	3 (1-4) <sup>**</sup>	3 (1-4) <sup>**</sup>	3 (1-4) <sup>**</sup>	2 (1-3) <sup>**#</sup>

SRTDD data are presented as medians (range). All other data are presented as means  $\pm$  SEM.

KW, kidney weight; BW, body weight; SCD, score of crystallization degree; SRTDD, score of renal tubule dilatation degree.

\*  $P < 0.05$ , \*\*  $P < 0.01$  vs. Group A.

#  $P < 0.05$ , ##  $P < 0.01$  vs. Group B.

\*  $P < 0.05$ , \*\*  $P < 0.01$  vs. NC group

#  $P < 0.05$ , ##  $P < 0.01$  vs. M group

$\Delta$   $P < 0.05$ ,  $\Delta\Delta$   $P < 0.01$  vs. M + TFL group

\* P < 0.05, \*\* P < 0.01 vs. NC group.

# P < 0.05, ## P < 0.01 vs. M group.

\* P < 0.05, \*\* P < 0.01 vs. NC group,

# P < 0.05, ## P < 0.01 vs. M group

(A) Western blot analyses showing the protein expression levels of Nrf2, HO-1, and NQO-1 after transfecting Nrf2 siRNA into HK-2 cells. (B) Relative density of total Nrf2 expression with  $\beta$ -actin as the loading control. (C) Relative density of intracellular Nrf2. (D) Relative density of nuclear Nrf2. (E) Relative density of HO-1. (F) Relative density of NQO-1. Values are presented as means  $\pm$  SEM.

\* P < 0.05, \*\* P < 0.01.

## 4. Discussion

The mechanism of renal calculus formation is very complex. However, a growing number of studies have shown that RTEC injury is an important cause of renal calculus formation<sup>20</sup>. Thus, it is important to study the interaction between CaOx crystals and RTECs to understand the formation and pathogenesis of renal calculi. When CaOx crystals interact with RTECs they cause oxidative damage, which leads to cell death and damage to nearby cells<sup>21</sup>. The damaged cells gradually become fragments, which then become nucleation centers that allow further crystal aggregation, ultimately causing the cascade reaction for stone formation. Farrell et al.<sup>22</sup> summarized the pathophysiological process of renal calculus formation. Specifically, CaOx crystals act on RTECs and activate NADPH oxidase. The abnormal increase in ROS leads to mitochondrial death, caspase-3 activation, cell damage, structural changes in membrane phosphatidylserine, and renal crystal adhesion. A positive feedback loop between cellular OS induced damage and crystal adhesion forms a vicious cycle that accelerates renal calculus formation. In the damaged area, crystal adhesion was facilitated, inducing more oxidative damage, and increasing cell death. Thus, reducing CaOx-induced OS in RTECs can possibly prevent renal calculus formation.

We showed here that CaOx crystal treatment significantly decreased SOD activity and increased MDA content in HK-2 cells. Treating rats with 0.5% glycol and 2% ammonium chloride also decreased SOD activity; however, it increased the MDA levels in rat kidney tissues, suggesting that CaOx stones can induce OS in renal tissue. By treating CaOx-mediated OS in HK-2 cells with TFL, we observed significantly increased SOD activity and decreased MDA content, thus reducing the OS induced by CaOx crystals. In addition, TFL reduced the renal tissue damage and CaOx crystallization in model rats. These observations indicate that the preventive effects of TFL on CaOx stones might be closely associated with reduced OS in the renal tissue. However, the underlying mechanism remained unclear. Thus, we investigated whether the protective effects of TFL on OS in renal tissue occur by the regulation of the Nrf2/ARE pathway, thus preventing renal calculus formation.

The Nrf2/ARE pathway is an important endogenous anti-OS pathway used for defense against oxidative and electrophilic stress. Nrf2 has antioxidant effects and is an important target in the prevention and treatment of OS-related diseases<sup>10</sup> thereby maintaining the stability of the intracellular environment and immune surveillance. Previous studies have shown that some flavonoids are activators of Nrf2 and exert antioxidant effects by activating the Nrf2 signaling pathway<sup>17</sup>. After confirming that TFL reduced OS in renal tissue using *in vitro* and *in vivo* CaOx stone models, we investigated the effect of TFL on the Nrf2-ARE pathway. *In vitro* experiments revealed that, after HK-2 cells were treated with CaOx crystals, activated Nrf2 was recruited to the nucleus. Nrf2 binding with the ARE initiates downstream gene transcription, thereby upregulating HO-1 and NQO-1 expression and activating an anti-OS reaction. TFL treatment further increased nuclear Nrf2 content, and increased HO-1 and NQO-1 protein expression in HK-2 cells treated with CaOx. In addition, TFL treatment significantly increased SOD activity and decreased MDA content in CaOx crystal-treated HK-2 cells. These results indicate that the protective effect of TFL on OS may be by activating the Nrf2/ARE pathway.

Based on these results, Nrf2 siRNA treatment was undertaken to uncover whether the protective effects of TFL on OS involved activating the Nrf2/ARE pathway. SiRNA, also known as silent RNA and noncoding RNA, is a small RNA fragment with a specific length and sequence that can combine with the mRNA expressed by genes in the form of single strand, inducing the degradation of this mRNA<sup>23</sup> and resulting in silencing of target gene expression. Transfecting Nrf2 siRNA into HK-2 cells caused the expression of Nrf2, HO-1, and NQO-1 to decrease significantly, verifying that the transfection was successful. Furthermore, Nrf2 siRNA treatment significantly prevented TFL-induced nuclear Nrf2, HO-1, and NQO-1 upregulation in CaOx-treated HK-2 cells. Nrf2 siRNA also markedly prevented the effect of TFL on SOD activity. This indicates that there was no effect of TFL on CaOx crystal-induced OS after Nrf2 siRNA treatment. Thus, it can be said that the protective effect of TFL on CaOx-induced OS in renal tissue is closely related to the Nrf2/ARE pathway.

## 5. Conclusion

Taken together, our findings indicate that TFL increased nuclear Nrf2, HO-1, and NQO-1 expression, and SOD activity in CaOx-treated HK-2 cells and rat models. Further, TFL decreased the MDA content and reduced CaOx-induced OS, thereby decreasing RTEC apoptosis. Overall, TFL prevented CaOx stone formation *in vivo* and *in vitro*. These results illustrate that the protective effect of TFL on OS induced by CaOx is closely associated with the Nrf2/ARE pathway. Thus, we have clarified the mechanisms responsible for the effects of TFL in the prevention and treatment of renal calculi.

## Abbreviations

TFL: Total flavonoids from *Lysimachia christinae*; CaOx: Calcium oxalate; Nrf2/ ARE: Nuclear factor-E2 related factor 2/Antioxidant response element; HO-1:Hemeoxygenase-1; NQO-1:NAD(P)H quinone oxidoreductase 1; OS: Oxidative stress; SOD:Superoxide dismutase; MDA: Malondialdehyde; DPT:

Diphenyleneiodonium; MTT: 3-(4,5-dimethylthiazol-2-yl)-2,5-diphenyltetrazolium bromide tetrazolium;  
RTEC: Renal tubule epithelial cell.

## Declarations

### Acknowledgements

Not applicable

### Authors' contributions

TT and JW conceived and designed the study. JW, JC, JH and TT conducted the experiments. BL, XH, JF, WH and QH provided the technical support and advices for the study. JW wrote the manuscript, TT revised the manuscript. All authors contributed to the review and the approval of the final manuscript. All authors read and approved the final manuscript

### Funding

This work was supported by the grants from National Natural Science Foundation of China (grant number 82074433); the Natural Science Foundation of Zhejiang Province(grant number LY18H05004); the Zhejiang Administration of traditional Chinese Medicine(grant number 2014ZQ015).

### Availability of data and materials

The datasets used and/or analyzed during the current study are available from the corresponding author on reasonable request.

### Ethics approval and consent to participate

The animal experiments were approved by the Animal Experimental Ethics Committee of Zhejiang Chinese Medical University

### Consent for publication

Not applicable

### Competing interests

The authors declare no competing interests.

## References

1. Lieske JC, Rule AD, Krambeck AE, Williams JC, Bergstralh EJ, Mehta RA, et al. Stone composition as a function of age and sex. Clin J Am Soc Nephrol 2014; 9 (12): 2141-2146. doi: 10.2215/CJN.05660614.

2. Attanasio M. The genetic components of idiopathic nephrolithiasis. *Pediatr Nephrol* 2011; 26 (3): 337-346. doi: 10.1007/s00467-010-1562-6.
3. Parvin M, Shakhssalim N, Basiri A, Miladipour AH, Golestan B, Mohammadi Torbati P, et al. The most important metabolic risk factors in recurrent urinary stone formers. *Urol J* 2011; 8 (2).
4. Khan SR. Renal tubular damage/dysfunction: key to the formation of kidney stones. *Urol Res* 2006; 34 (2): 86-91. doi: 10.1007/s00240-005-0016-2.
5. Tsujihata M. Mechanism of calcium oxalate renal stone formation and renal tubular cell injury. *Int J Urol* 2008; 15 (2): 115-120. doi: 10.1111/j.1442-2042.2007.01953.x.
6. Khan SR, Canales BK. Unified theory on the pathogenesis of Randall's plaques and plugs. *Urolithiasis* 2015; 43 Suppl 1 109-123. doi: 10.1007/s00240-014-0705-9.
7. Fasano JM, Khan SR. Intratubular crystallization of calcium oxalate in the presence of membrane vesicles: an in vitro study. *Kidney Int* 2001; 59 (1): 169-178. doi: 10.1046/j.1523-1755.2001.00477.x.
8. Thamilselvan S, Byer KJ, Hackett RL, Khan SR. Free radical scavengers, catalase and superoxide dismutase provide protection from oxalate-associated injury to LLC-PK1 and MDCK cells. *J Urol* 2000; 164 (1): 224-229.
9. Poljsak B, Šuput D, Milisav I. Achieving the balance between ROS and antioxidants: when to use the synthetic antioxidants. *Oxid Med Cell Longev* 2013; 2013 956792. doi: 10.1155/2013/956792.
10. Abed DA, Goldstein M, Albanyan H, Jin H, Hu L. Discovery of direct inhibitors of Keap1-Nrf2 protein-protein interaction as potential therapeutic and preventive agents. *Acta Pharm Sin B* 2015; 5 (4): 285-299. doi: 10.1016/j.apsb.2015.05.008.
11. Pajares M, Cuadrado A, Rojo AI. Modulation of proteostasis by transcription factor NRF2 and impact in neurodegenerative diseases. *Redox Biol* 2017; 11 543-553. doi: 10.1016/j.redox.2017.01.006.
12. Frijhoff J, Winyard PG, Zarkovic N, Davies SS, Stocker R, Cheng D, et al. Clinical Relevance of Biomarkers of Oxidative Stress. *Antioxid Redox Signal* 2015; 23 (14): 1144-1170. doi: 10.1089/ars.2015.6317.
13. Ratliff BB, Abdulmahdi W, Pawar R, Wolin MS. Oxidant Mechanisms in Renal Injury and Disease. *Antioxid Redox Signal* 2016; 25 (3): 119-146. doi: 10.1089/ars.2016.6665.
14. Zhu J, Wang Q, Li C, Lu Y, Hu H, Qin B, et al. Inhibiting inflammation and modulating oxidative stress in oxalate-induced nephrolithiasis with the Nrf2 activator dimethyl fumarate. *Free Radic Biol Med* 2019; 134 doi: 10.1016/j.freeradbiomed.2018.12.033.
15. Wang ZJ, Dai B, Wang FM. Microwave Technique Extraction and Determination of Total Flavonoids and Polysaccharides in *Lysimachia Christinae* Hance. *Chinese Journal of Modern Applied Pharmacy* 2008; (S1): 621-622.
16. Wu N-H, Ke Z-Q, Wu S, Yang X-S, Chen Q-J, Huang S-T, et al. Evaluation of the antioxidant and endothelial protective effects of *Lysimachia christinae* Hance (Jin Qian Cao) extract fractions. *BMC Complement Altern Med* 2018; 18 (1): 128. doi: 10.1186/s12906-018-2157-1.

17. Zhou MX. Investigation on Natural Antioxidants Targeting Nrf2 Signaling Pathway [D]: Shangdong University; 2018.
18. Tao TT, Lv BD, Huang XJ, Fu J, Ma YF. Study on the total flavone extract of lysimachia on calcium oxalate stone formation in rats. *China Modern Doctor* 2016; 54 (18): 30-33.
19. Tao TT, Zhao F, Ye MY, Lv BD, Fu J. Effect of Total Flavonoids from Christina Loosestrife (*Lysimachia Christinae*) on Osteopontin expression in renal tissue of calcium oxalate stone model rats. *Zhejiang Journal of Integrated Traditional Chinese and Western Medicine* 2019; 29 (08): 623-626+703.
20. Narula S, Tandon S, Singh SK, Tandon C. Kidney stone matrix proteins ameliorate calcium oxalate monohydrate induced apoptotic injury to renal epithelial cells. *Life Sci* 2016; 164 23-30. doi: 10.1016/j.lfs.2016.08.026.
21. Oliveira LCBP, Queiroz MF, Fidelis GP, Melo KRT, Câmara RBG, Alves MGCF, et al. Antioxidant Sulfated Polysaccharide from Edible Red Seaweed is an Inhibitor of Calcium Oxalate Crystal Formation. *Molecules* 2020; 25 (9): doi: 10.3390/molecules25092055.
22. Farrell G, Huang E, Kim SY, Horstkorte R, Lieske JC. Modulation of proliferating renal epithelial cell affinity for calcium oxalate monohydrate crystals. *J Am Soc Nephrol* 2004; 15 (12): 3052-3062. doi: 10.1016/j.redox.2017.01.006.
23. Crooke ST, Witztum JL, Bennett CF, Baker BF. RNA-Targeted Therapeutics. *Cell Metab* 2018; 27 (4): 714-739. doi: 10.1016/j.cmet.2018.03.004.

## Figures

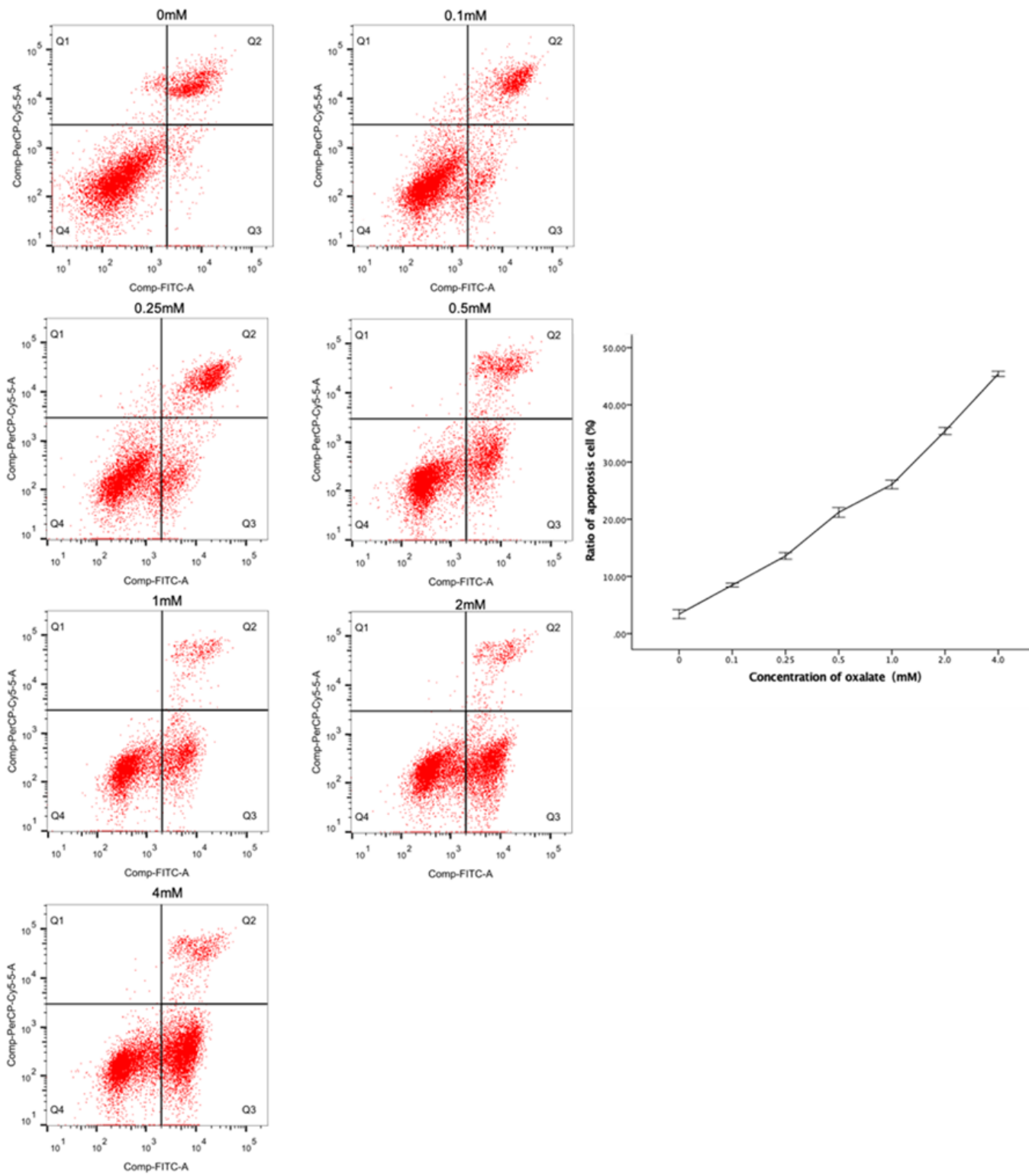


**Figure 1**

Effects of different concentrations of CaOx on HK-2 cell apoptosis

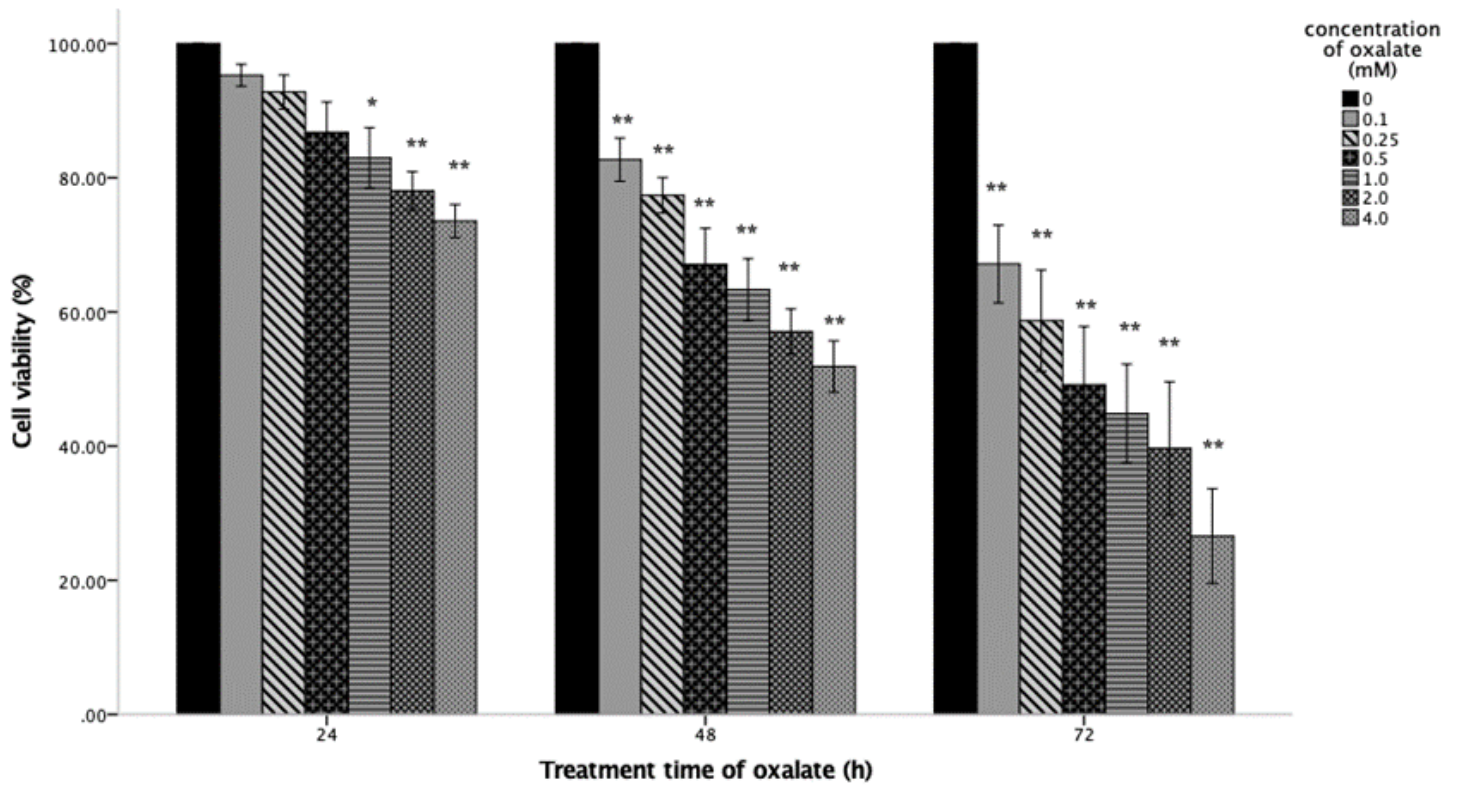
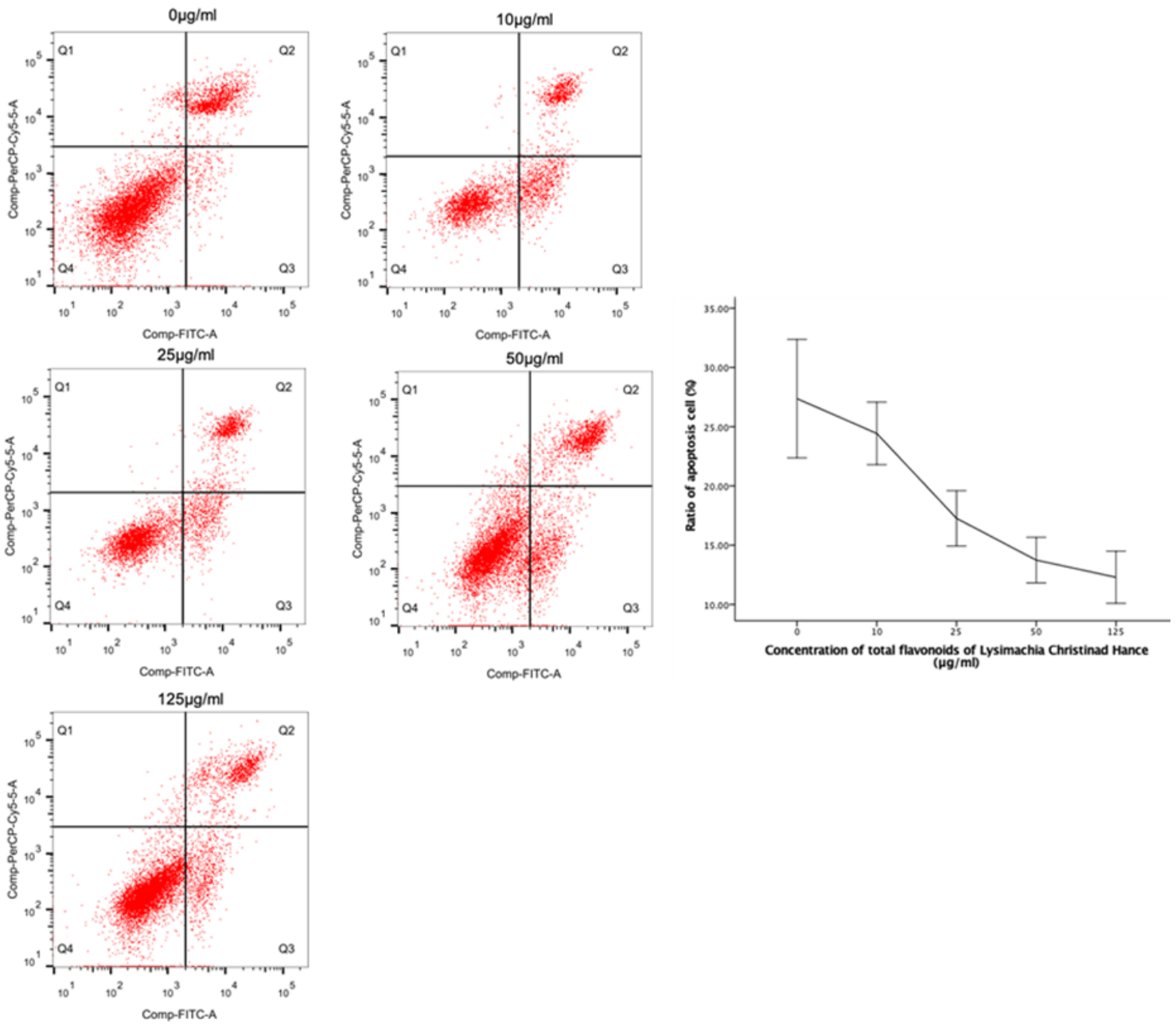


Figure 2

Effects of different concentrations of CaOx crystals on the survival of HK-2 cells



**Figure 3**

Effects of different concentrations of TFL on HK-2 cell apoptosis induced by CaOx crystals

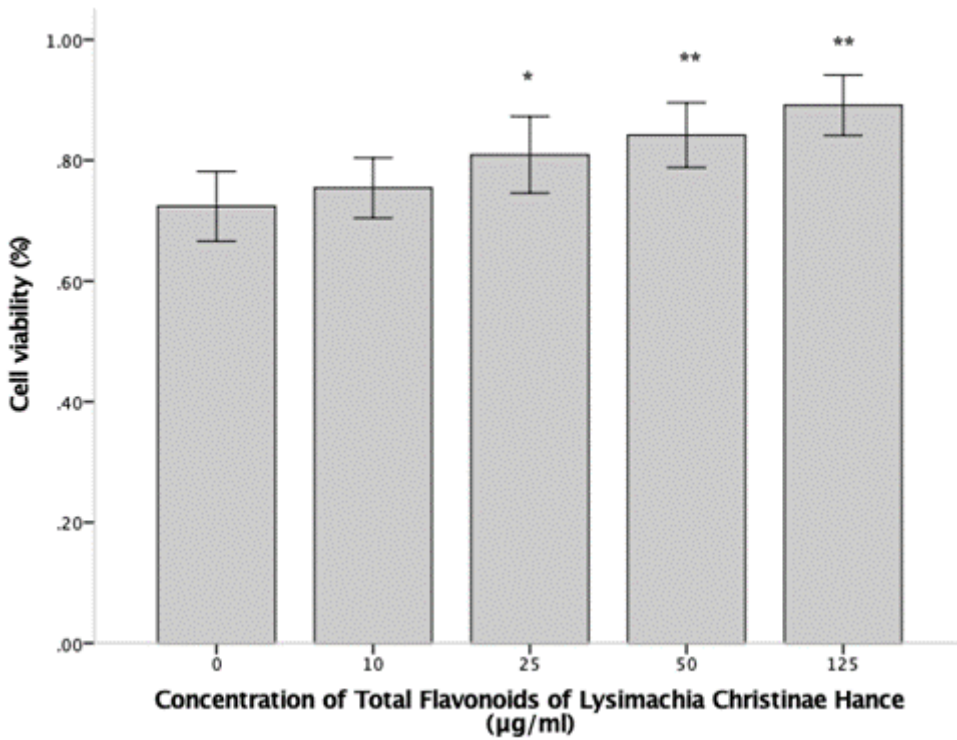


**Figure 4**

Effect of different concentrations of c CaOx on the viability of HK-2 cells

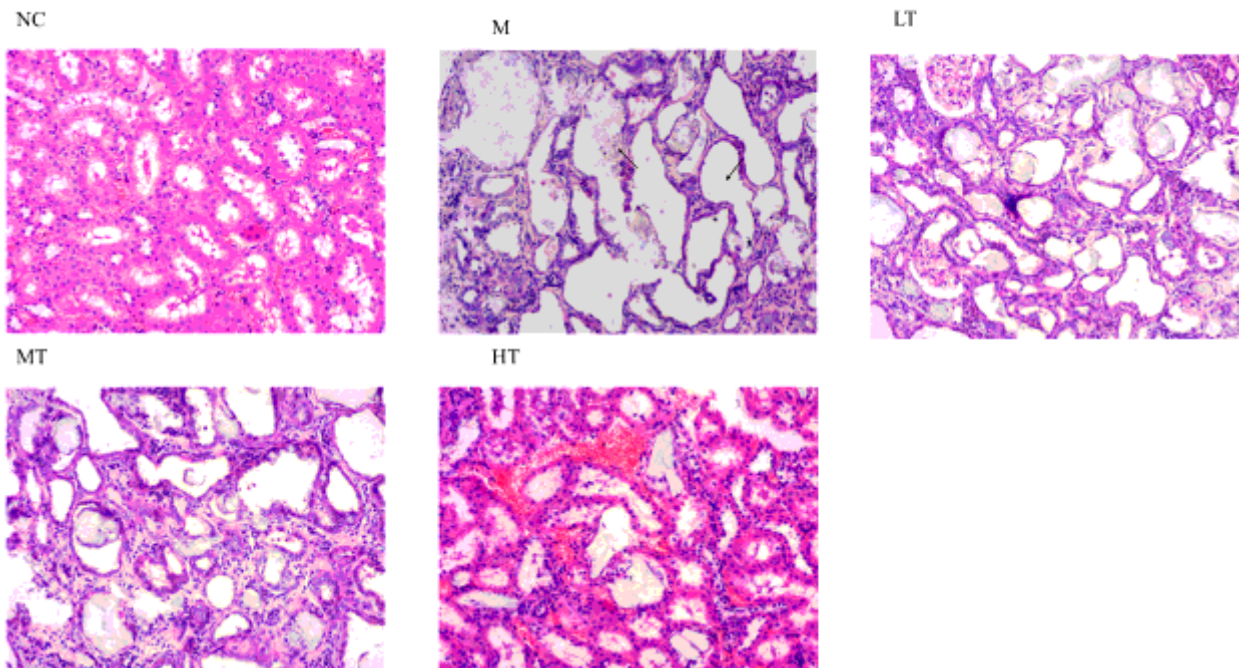


**Figure 5**

Representative hematoxylin/eosin staining of kidney tubules of the normal control (NC), CaOx stone model (M), M + low-dose TFL (LT), M + medium-dose TFL (MT), and M + high-dose TFL (HT) groups

(100× magnification).

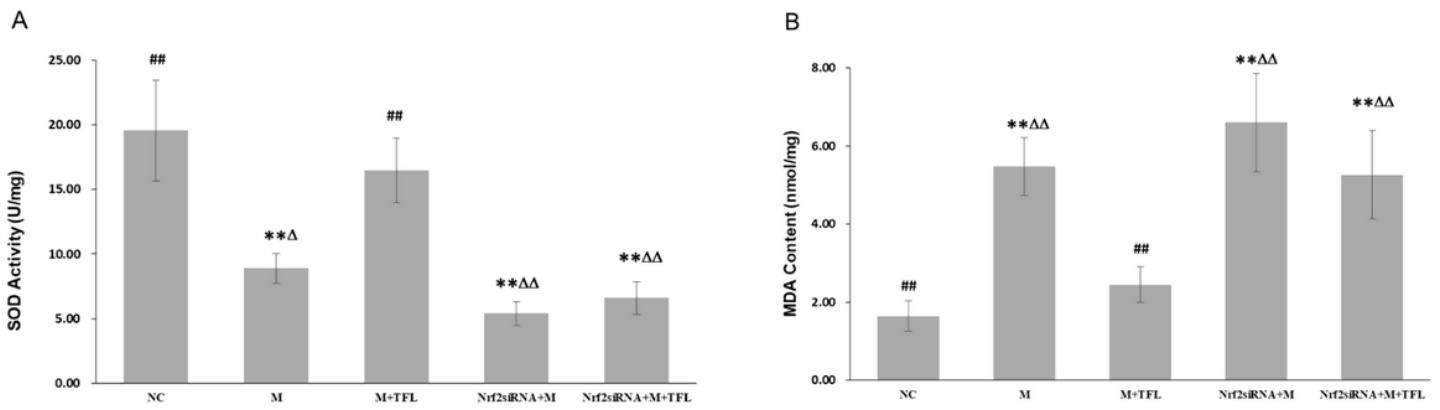


**Figure 6**

Effect of TFL and Nrf2 siRNA on CaOx stone-induced OS in HK-2 cells. (A) SOD activity in HK-2 cells. (B) MDA content in HK-2 cells.

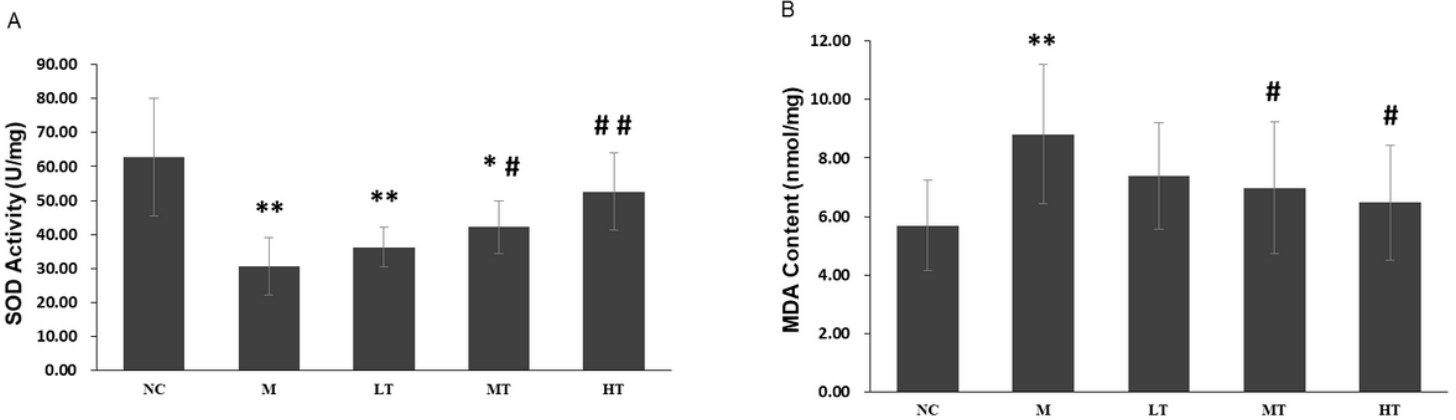


**Figure 7**

Effect of TFL on CaOx stone-induced OS in renal tissue. (A) SOD activity in renal tissue. (B) MDA content in renal tissue.

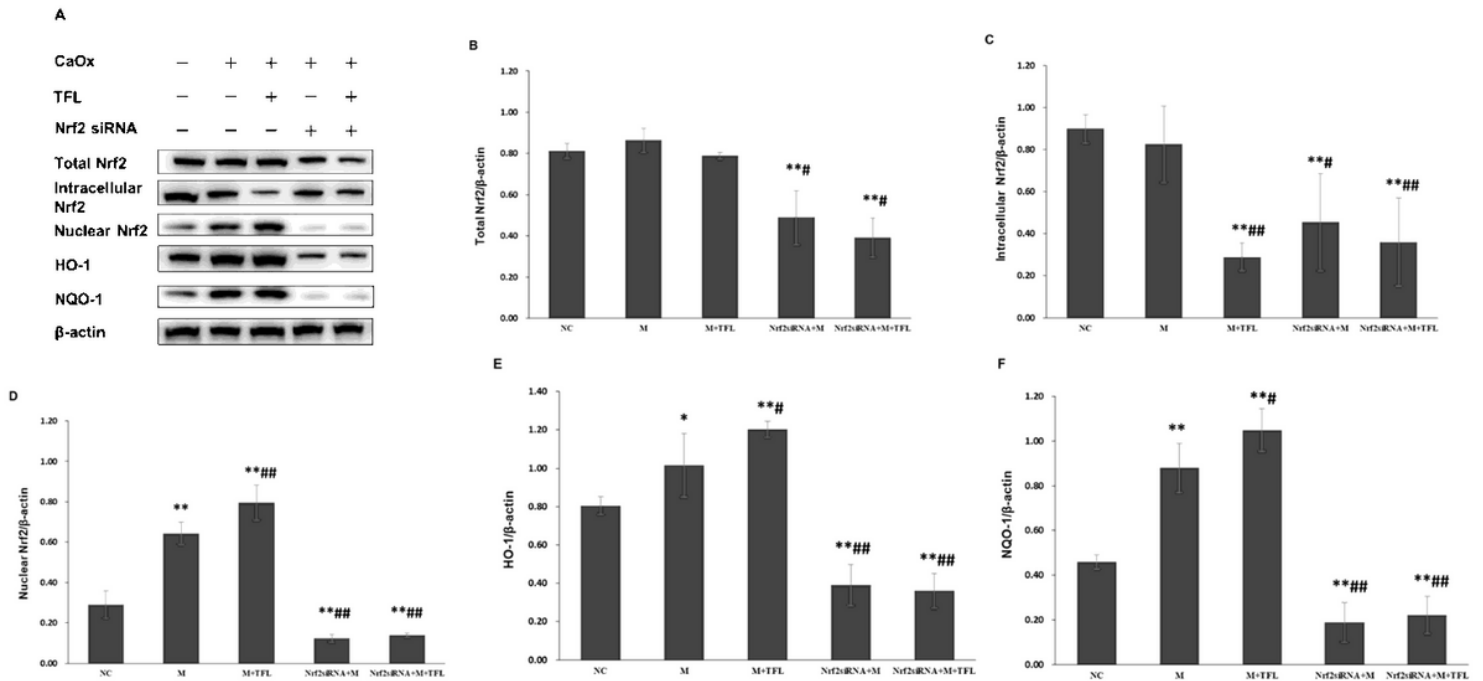


**Figure 8**

Effect of TFL and Nrf2 siRNA on the expression of Nrf2, HO-1, and NQO-1 in CaOx-treated HK-2 cells. (A) Western blot analyses showing the protein expression levels of Nrf2, HO-1, and NQO-1 after treatment with CaOx, TFL, and Nrf2 siRNA. (B) Relative density of total Nrf2 expression with  $\beta$ -actin as the loading control. (C) Relative density of intracellular Nrf2. (D) Relative density of nuclear Nrf2. (E) Relative density of HO-1. (F) Relative density of NQO-1. Values are presented as means  $\pm$  SEM.

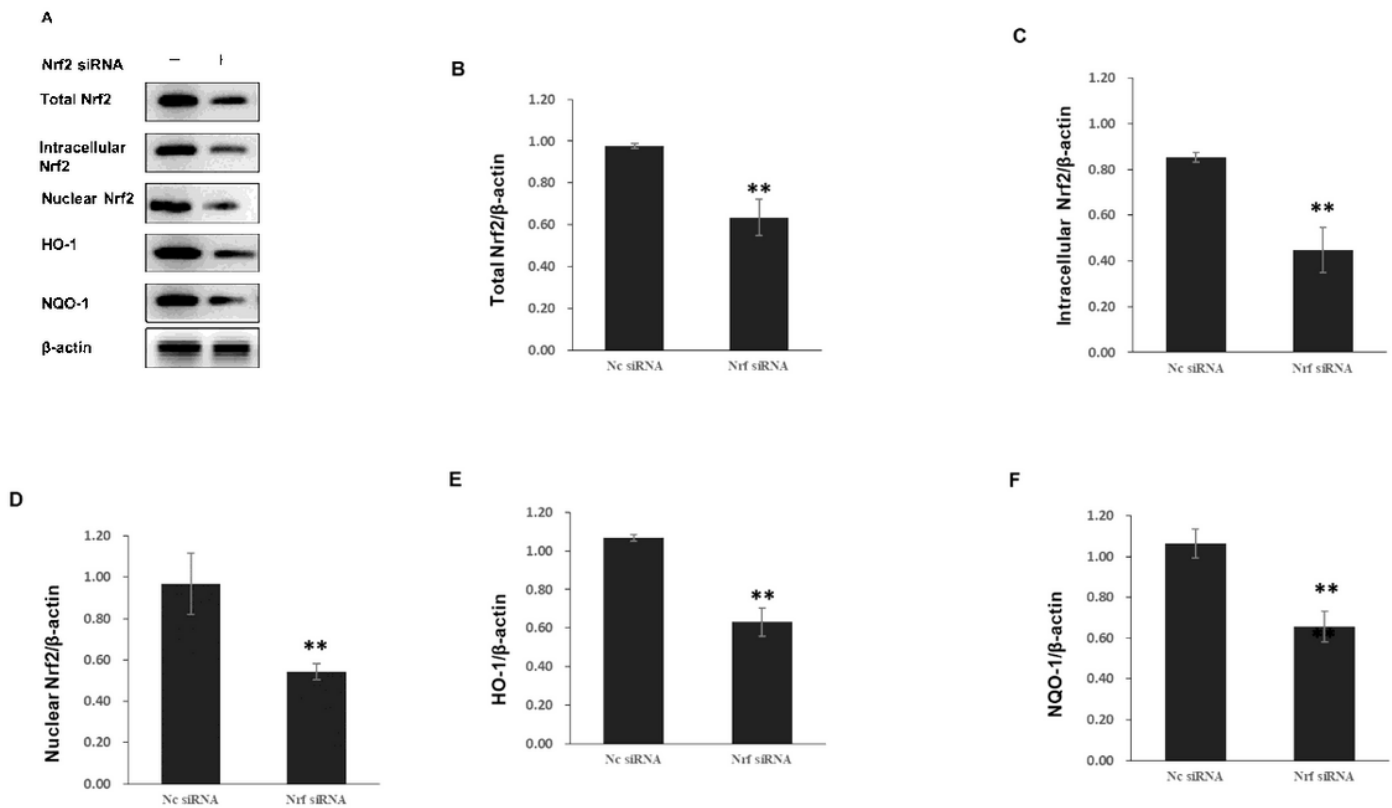


## Figure 9

Effect of Nrf2 siRNA on the expression of Nrf2, HO-1, and NQO-1 in HK-2 cells.